

Template-Controlled Assembly of Ditopic Catechol Phosphines: A Strategy for the Generation of Complexes of Bidentate Phosphines with Different Bite Angles

Samir H. Chikkali,^[a] Dietrich Gudat,^{*[a]} Falk Lissner,^[a] Mark Niemeyer,^[a, b] Thomas Schleid,^[a] and Martin Nieger^[c]

Abstract: A rational approach to the synthesis of heterobi- or -trimetallic complexes based upon self-assembly of a flexible ditopic catechol-phosphine ligand with [(cod)PdCl₂] and simple metal halides such as GaCl₃, BiCl₃, SnCl₄, or ZrCl₄ is described. All products were characterized by spectroscopic and analytical data and single-crystal X-ray diffraction studies. The molecular structures can be described in terms of *cis*-configured palladium complexes with supramolecular bisphosphine li-

gands that are formed by the assembly of two phosphine catecholate fragments on a main group/transition metal template. Of particular interest are the distinct decreases in P-Pd-P bite angles and P...P distances between the ligating atoms with increasing covalent radii of the templates. The range of these varia-

tions is of a magnitude similar to that of the geometrical changes in known families of complexes containing molecular bidentate ligands. Solution NMR studies give further evidence that in several cases the μ_2 -bridging coordination of two of the catechol oxygen atoms in the template complexes is broken under the influence of donor solvents, thus allowing the supramolecular ligand to be switched between tetradentate -O₂P₂ and bidentate -P₂ coordination modes.

Keywords: bite angles • heterogeneous catalysis • palladium • self-assembly • templates

Introduction

Over the last few decades, bidentate ligands have been widely employed to improve the selectivities, activities, and stabilities of metal-complex-based homogeneous catalysts.^[1] The key to optimization of the performance of a certain specimen in a catalytic reaction is to adjust the electronic and steric properties of the ligands, often categorized in

terms of descriptors such as the cone angle or the “natural bite angle”.^[2] However, as one cannot easily predict the activity and selectivity of a metal complex, catalyst improvement still relies to a large extent on a trial-and-error strategy and may require the screening of a whole family of tailored ligands. To be successful, such an approach calls not only for reliable assays to test catalysts but also for the development of efficient synthetic methods to provide the needed ligands and complexes. Some progress in this direction has been made in the form of the replacement of tedious multistep protocols for the preparation of special bisphosphines^[3] by modular syntheses permitting rational construction of whole ligand families with structurally different molecular backbones.^[4] Another, perhaps even more widely applicable, approach is based on the introduction of supramolecular bidentate ligands that form spontaneously (by “self-assembly”) upon mixing of two suitably functionalized monodentate ligands.^[5] The chelating backbone is in this case formed either through direct intermolecular interaction between complementary binding motifs in both fragments, or by secondary coordination of both building blocks to a common template. Examples of the first approach include the pairing of ligand components through hydrogen

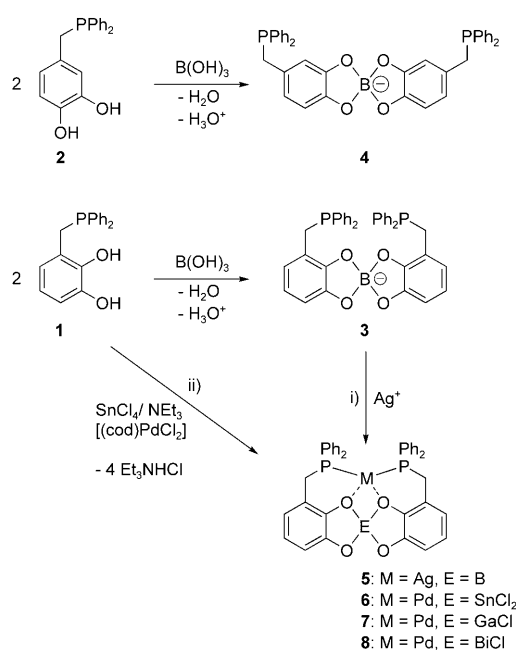
[a] Dr. S. H. Chikkali, Prof. Dr. D. Gudat, Dr. F. Lissner, Priv.-Doz. Dr. M. Niemeyer, Prof. Dr. T. Schleid
Institut für Anorganische Chemie, Universität Stuttgart
Pfaffenwaldring 55, 70569 Stuttgart (Germany)
Fax: (+49) 711-6856-4241
E-mail: gudat@iac.uni-stuttgart.de

[b] Priv.-Doz. Dr. M. Niemeyer
Current address:
Institut für Anorganische und Analytische Chemie
Johannes-Gutenberg-Universität
Duesbergweg 10–14, 55128 Mainz (Germany)

[c] Dr. M. Nieger
Laboratory of Inorganic Chemistry
University of Helsinki
A. I. Virtasen aukio 1, Helsinki (Finland)

bonding interactions.^[6] Template-based supramolecular ligands have been assembled through the binding of ditopic fragments to a catalytically inactive metal ion such as Zn^{2+} ,^[7,8] or by anion sequestering.^[9]

We have recently described the simple synthesis of the phosphines **1** and **2** (Scheme 1),^[10] flexible ditopic ligands with binding sites at the phosphorus atom and the catechol unit. These building blocks allow the assembly of template-centered, anionic bisphosphines **3** and **4**, of which **3** is capable of forming a chelate complex **5** with a transition metal (Scheme 1i).^[11] In a preliminary account, it was further reported that the construction of a template-based bidentate ligand and its complexation to yield **6** can be accomplished in one-step manner in a self-assembling process (Scheme 1ii).^[12] Because this aggregation relies heavily on the reversibility and kinetic lability of the formed tin-(template)-oxygen bonds, the template-based bisphosphine moiety may be considered a supramolecular ligand. The available results show that the assembled ligand entities are sufficiently rigid to display specific bite angles^[11] and exhibit interesting features such as hemilabile coordination behavior.^[12] Correspondingly, it might be expected that self-assembly of the same ligand building block on templates of different size and coordination geometry should be utilizable to construct a series of bisphosphine chelates with variable geometric predispositions of the donor moieties, thus allowing fine-tuning of the steric bulk and, in particular, the bite angle of the chelating ligand by directed adjustment of the shape of the supramolecular backbone. In order to validate this hypothesis, we have explored in some detail the synthesis of complexes through self-assembly of **1**, a palladium precursor, and different templates derived from tri- or tetravalent main group elements or transition metals, respectively.



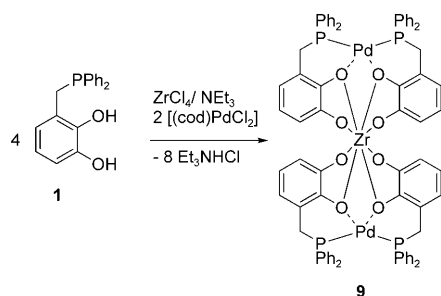
Scheme 1.

Results and Discussion

Assembly of template complexes: The catechol phosphine **1** was readily synthesized as reported earlier, by hydrophosphination, followed by the reduction of the resultant phosphine oxide with excess LiAlH_4 .^[10] One-step syntheses of template complexes were generally carried out by treatment of mixtures of **1** (2 equiv), $[(\text{cod})\text{PdCl}_2]$ (1 equiv; cod = cycloocta-1,5-diene), and a suitable main group element or transition metal chloride (1 equiv), which served as the source of the template, with excess triethylamine (2.5 to 5 equiv). The template sources used included various chlorides of tri- and tetravalent main group elements (AlCl_3 , GaCl_3 , SiCl_4 , SnCl_4 , BiCl_3), as well as ZrCl_4 , chosen because of their known ability to form stable catecholate complexes.^[13–15] Furthermore, aluminium and gallium are larger congeners of boron, whereas Ga^{III} , thanks to its similar ion radius, is a mimic of Fe^{III} , an important component in biological^[16] and redox processes.^[17] Last, but not least, zirconium oxide materials are receiving increasing interest as supports for palladium-based cross-coupling catalysts^[18] and with regard to the application of tin compounds as cocatalysts during palladium-catalyzed carbonylation,^[19] Pd/Sn bimetallic complexes might have interesting potential in catalysis.

The individual reactions were routinely carried out in DMF, which turned out to provide optimum solubility for all components, and the levels of conversion were monitored by ^{31}P NMR spectroscopy. Reactions involving gallium and bismuth trichlorides showed quantitative formation of single complexes within a few hours at ambient temperature. The products were precipitated by addition of diethyl ether and isolated in good yields (70%) after filtration and drying in vacuum; identification as the bimetallic complexes **7** and **8** (Scheme 1) was achieved by means of analytical and spectroscopic data and single-crystal X-ray diffraction studies (see below). The reaction involving tin tetrachloride was less selective, and after 24 h had produced a mixture of several products from which complex **6** was isolated in 40% yield after a similar workup procedure.^[12] In attempts to optimize the reaction conditions it was found that the highest level of conversion to the desired template complex was obtained when the reaction temperature was raised to 60°C ; performing the reaction under these conditions allowed **6** to be isolated in 60% yield after the same workup procedure.

The reaction with zirconium tetrachloride was conducted at room temperature in the presence of Cs_2CO_3 (1.3 equiv) as base. The product, which was isolated in 60% yield after precipitation from a ternary DMF/ CH_2Cl_2 /diethyl ether mixture, was identified by its analytical and spectroscopic data and a single-crystal X-ray diffraction study as the trinuclear complex **9** (Scheme 2), in which the zirconium atom acts as a double template spanning two bisphosphine moieties. Interestingly, this species was likewise obtained as the only isolable product during attempts to prepare a monopalladium template complex with a structure similar to those of **6**–**8** from the starting bis(cyclopentadienyl)zirconium dichlor-



Scheme 2.

ide. The cleavage of the organometallic ligand, which is presumably lost as cyclopentadiene, contrasts with the assembly of a $\text{Me}_2\text{Sn}(\text{L})_2\text{Pd}$ complex on Me_2SnCl_2 as template precursor^[12] and indicates that the π -bonded Cp ligand is more vulnerable to electrophilic attack than a methyl substituent. The reactions involving aluminium and silicon chlorides as templates were messy and did not yield isolable products; these reactions were therefore not pursued further.

The isolated template complexes are dark red, high-melting crystalline materials that are relatively stable towards air and moisture. All the compounds are only sparingly soluble in solvents of medium polarity such as CH_2Cl_2 or acetonitrile, but dissolve in DMF and DMSO. The identities of the isolated complexes were unambiguously derived from NMR data and X-ray diffraction studies, which are discussed further below. Interesting insight into the solution structures and solvation properties was obtained from the results of positive-mode electrospray ionization mass spectra (ESI-MS). The spectrum of a methanol solution of the gallium complex **7** displayed—beside signals arising from the pseudomolecular ions $[\text{M}+\text{Na}]^+$ (m/z : 847.0, 40%^[20]) and $[\text{M}+\text{H}]^+$ (m/z : 825.0, 5%)—as the main signal a peak attributable to a cation $[\text{M}+\text{H}+\text{MeOH}]^+$ (m/z : 857.0, 100%). The appearance of this ion suggests that the complex exists in solution as a solvate that contains one rather tightly bound solvent molecule, presumably as an additional gallium-bound ligand, which thus completes the preferred octahedral coordination sphere of this element.

The corresponding spectrum of the bismuth complex **8** displays—beside a weak signal of a pseudomolecular ion $[\text{M}+\text{Li}]^+$ (m/z : 969.0, 10%)—a peak of a cation $[\text{M}-\text{Cl}]^+$ (m/z : 927.0, 100%) formed by loss of a chloride. Particular interesting is the ESI-MS of the zirconium complex **9**, which shows a peak at m/z : 1713.0 (100%) attributable to a cation $[\text{M}+2\text{DMF}+\text{K}]^+$ whereas the pseudomolecular ion $[\text{M}+\text{H}]^+$ (m/z : 1529.0) is hardly visible; an additional weak signal (m/z : 841.0, 10%) is attributed to a monotemplate complex $[\text{Pd}+2\text{L}+\text{Zr}+\text{OME}]^+$ ($\text{LH}_2=\mathbf{1}$) presumably arising from partial solvolysis of the trinuclear complex. The solvent molecules in the most abundant ion stem from DMF added in this case to increase the solubility, and the observation of this species emphasizes the capability of the template complex to coordinate additional solvent molecules in solution.

Single-crystal X-ray diffraction studies: Crystalline samples of complexes **6–9** that were suitable for single-crystal X-ray diffraction studies were obtained by recrystallization from appropriate solvent mixtures (see Experimental Section). The resulting crystals were obtained as solvates with one to four co-crystallized solvent molecules per complex. In the cases of **6–8**, the solvates are formed by occlusion of halo-carbon molecules, which exhibit weak $\text{CH}\cdots\text{Cl}$ hydrogen bonding interactions with the peripheral E–Cl bonds in the complexes; these contacts, however, are not considered to induce significant structural distortions. The chloride-free complex **9** recrystallized with four molecules of DMF that do not show significant intermolecular interactions. Graphical representations of the molecular structures of the complexes are shown together with listings of the most important metric parameters in Figures 1–4. The molecular complexes in the crystals of **6** (space group P_2/c) and **9** (space group C_2/c) lie on the crystallographic C_2 axes in monoclinic unit cells, whereas the molecules in crystals of **7** (space group $P_{21/n}$) and **8** (space group $P_{21/c}$) exhibit no further crystallographically imposed symmetry.

All complexes contain as a common structural element a bis(catechol phosphine)-palladium moiety in which the metal atom is coordinated by two P,O-chelating phosphine fragments to give a distorted square-planar geometry with a *cis* arrangement of the phosphorus and oxygen atoms. The catechol oxygen atoms either of one (in **6–8**) or of two (in **9**) of these units bind in a doubly O,O-chelating fashion to the template E, the coordination sphere of which is completed by additional ancillary ligands. One oxygen atom in each catecholate moiety thus ends up as terminal donor that binds exclusively to the template, whereas the second oxygen atom acts as a μ_2 -bridging donor both to the template E and to palladium. A consequence of this arrangement is the creation of a polycyclic framework consisting of a central, diamond-shaped EO_2Pd ring formed by the Lewis acid centers and the μ_2 -bridging oxygen atoms, together with two E,O,O- and two Pd,O,P-based chelate rings, each type of which flanks two adjacent edges of the central diamond. The metric parameters in the Pd-centered P,O-chelate rings in all complexes do not differ significantly, and the Pd–P (2.221–2.256 Å) and Pd–O (2.056–2.089 Å) bond lengths fall into the ranges reported in the literature for comparable complexes (Pd–P 2.25 ± 0.02 Å,^[21] Pd–(μ_2 -O) 2.02–2.17 Å^[22]). The P–Pd–O angles in the chelate rings (91.5–93.7°) are close to the ideal bond angle of 90° in a square-planar complex.

The most prominent structural differences in the complexes studied arise from the presence of templates of different size and different coordination number (5 to 8). The lowest coordination number is observed for the gallium atom in **7** (Figure 1), which also has the smallest ion radius of all template atoms in the complexes studied, and features a single chlorine ligand beside the four oxygen atoms of two catecholate units. All five ligand atoms are arranged in a distorted square pyramidal geometry, in which the four oxygen atoms occupy the basal square. The Ga–O bonds to

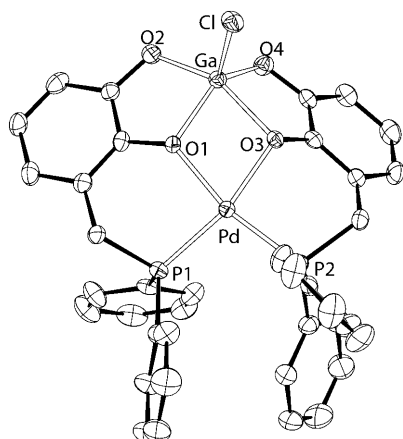


Figure 1. Molecular structure of **7** (H atoms and solvent molecules omitted for clarity; 50% probability thermal ellipsoids); selected interatomic distances [Å] and angles [°]: Pd–P1 2.250(1), Pd–P2 2.248(1), Pd–O1 2.171(2), Pd–O3 2.080(3), Ga–O1 1.971(3), Ga–O2 1.915(3), Ga–O3 2.082(3), Ga–O4 1.881(2), Ga–Cl 2.188(1); P1–Pd–P2 101.8(1), O1–Pd–O3 74.3(1).

the μ_2 -bridging oxygen atoms (1.97–2.08 Å) are, as would be expected, longer than those to the terminal ones (1.88–1.91 Å). The displacement of the gallium atom by 0.8 Å from the basal plane of the pyramid reduces the sum of the O–Ga–O angles to 340° (relative to 360° in an ideal square pyramid) and helps to compensate some of the ring strain that arises from the geometric constraints in the polycyclic framework. This strain is presumably also responsible for the fact that the coordination geometry of the μ -bridging oxygen atoms deviates from the normally observed quasi-planar bonding situation^[23] and becomes distinctly pyramidal (sum of bond angles 322–349°), thus inducing a *trans* inclination of the catecholate-based chelate rings with respect to the central, planar GaO₂Pd ring. Interestingly, whereas hexa- and tetracoordinate gallium catecholate complexes are well known in the literature,^[24] there are very few reports on species with square pyramidal, pentacoordinate gallium atoms^[25], and although cluster compounds with palladium–gallium metal–metal bonds have recently been reported,^[26] it is worth mentioning that complex **7** is the first palladium–gallium heterodinuclear complex featuring this coordination geometry.

The tin atom in complex **6** (Figure 2) displays a strongly distorted octahedral coordination geometry in which the two chlorine atoms and the two pairs of oxygen atoms of the catecholate units occupy mutual *cis* positions. The most prominent deviations from regular octahedral geometry are characterized by the opening of the Cl–Sn–Cl' angle (104.3(1)°) and concomitant contraction of the opposite O1–Sn–O1' (73.5(1)°) angle, the enlargement of the O1–Sn–O2' angle (103.6(1)°), and the strong tilt of the O1–Sn–O1' plane out of an equatorial plane defined by the Sn and the O1/O1' and Cl/Cl' atoms. All distortions are easily explained as consequences of the large bite angles of the rigid chelating catecholate moieties in combination with the geometric con-

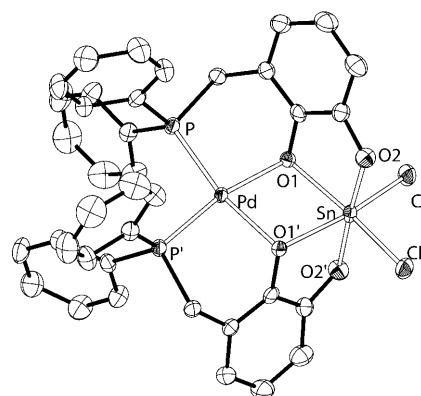


Figure 2. Molecular structure of **6** (H atoms and solvent molecules omitted for clarity; 50% probability thermal ellipsoids); selected interatomic distances [Å] and angles [°]: Pd–P 2.252(1), Pd–O1 2.088(2), Sn–O1 2.171(2), Sn–O2 2.033(3), Sn–Cl 2.390(1); P–Pd–P' 98.8(1), O1–Pd–O1' 77.0(1), O1–Pd–P 168.6(1), O1–Sn–O1' 73.5(1), Cl–Sn–Cl' 104.3(1), O2–Sn–O1 79.1(1), O2–Sn–Cl 91.5(1).

straints imposed by the polycyclic framework of the heterodinuclear complex. The second factor again produces a strictly pyramidal coordination at the μ_2 -bridging oxygen atoms (sum of the angles 323°) which induces a *trans*-bent arrangement of the exocyclic O–C bonds with respect to the planar SnO₂Pd ring and contrasts with the normally observed presence of planar μ_2 -bridging O atoms in heterodinuclear phenoxide or alkoxide complexes.^[23]

The bismuth complex **8** features the same molecular composition as **7**, but the larger template atom displays an additional secondary intermolecular interaction to a chlorine atom of a neighboring molecule, which induces a pairing of two molecular complexes to give a centrosymmetric dimer (Figure 3, crystallographic *C_i* symmetry). The bridging chlorine atoms show highly asymmetric coordination, with the “intramolecular” distance (Bi–Cl 2.766(2) Å) being distinctly shorter than the “intermolecular” one (Bi'–Cl 3.301(2) Å). This distortion indicates that the intermolecular interactions are rather weak, which is compatible with the results of the ESI-MS studies, in which no evidence for the persistence of the dimer in solution was obtained.

The four oxygen and two (including the secondary contact) chlorine atoms surrounding each bismuth form a strongly distorted octahedron in which the O2–Bi–O4 (85.7(2)°), O1–Bi–O3 (66.0(2)°), and Cl–Bi–Cl angles (77.6(1)°) are much smaller than the normal octahedral angles, thus leaving a large void between the chlorine and the O1 and O2 atoms, which is presumably occupied by the inert lone pair of electrons. Similar distortions were reported by Smith et al.^[14] and suggest that the bismuth atom in **8** is best described as having an effective coordination number of seven and a capped trigonal prismatic coordination geometry. The increased size of the template center in relation to **7** is naturally reflected in a lengthening of the μ_2 -O–Bi distances by some 0.4 Å. The coordination geometry of the μ_2 -bridging O1 and O3 atoms remains pyramidal (sum of bond angles 335–337°) but the bending of the two catecholate

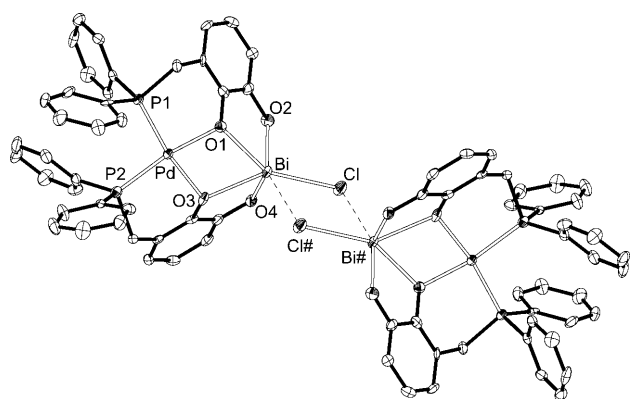


Figure 3. Dimeric molecular structure of **8** (H atoms and solvent molecules omitted for clarity; 50% probability thermal ellipsoids); selected interatomic distances [Å] and angles [°]: P1–Pd 2.256(2), P2–Pd 2.255(2), O1–Pd 2.073(5), O3–Pd 2.089(5), O1–Bi 2.458(5), O2–Bi 2.174(6), O3–Bi 2.439(5), O4–Bi 2.139(5), Cl–Bi 2.766(2), Cl#–Bi 3.301(2); P1–Pd–P2 97.1(1), O1–Bi–Cl 149.9(1), O2–Bi–Cl 89.5(2), O3–Bi–Cl 144.1(1), O4–Bi–Cl 83.3(2), O2–Bi–O4 85.7(2), O1–Bi–O3 66.0(2), Bi–Cl–Bi# 102.4(1), Cl–Bi–Cl# 77.6(1).

chelate rings relative to the central planar BiO₂Pd ring now occurs in a *cis* rather than a *trans* fashion as in **6** and **7**, thus imposing a local environment on the palladium atom that comes close to local C_s rather than C₂ symmetry.

The zirconium atom in complex **9** is octacoordinated by the oxygen atoms of four catecholate moieties and adopts a distorted square antiprismatic coordination geometry (Figure 4), which has precedence in other zirconium(IV) chelate complexes.^[27] The observation of Zr–O distances of 2.13–2.16 Å for terminal and 2.25–2.29 Å for μ₂-bridging oxygen atoms makes the central atom the largest template in all complexes studied, which accordingly results in the smallest bite angle for the chelating catecholate units (O–Zr–O 71°). The pyramidalization of the μ₂-bridging oxygen

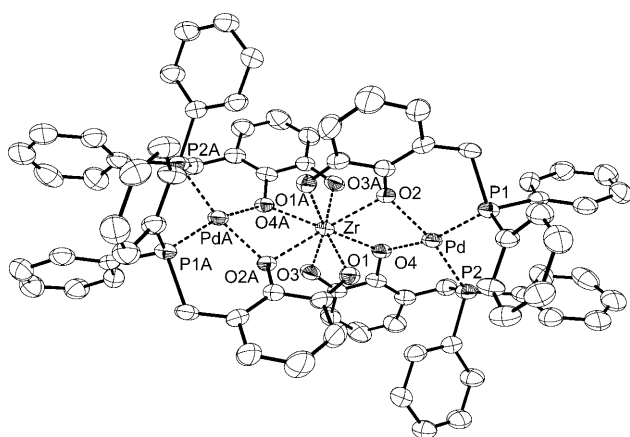


Figure 4. Molecular structure of **9** (H atoms and solvent molecules omitted for clarity; 50% probability thermal ellipsoids); selected interatomic distances [Å] and angles [°]: P1–Pd 2.223(2), P2–Pd 2.230(2), O2–Pd 2.060(3), O4–Pd 2.049(4), O1–Zr 2.154(4), O2–Zr 2.290(4), O3–Zr 2.135(4), O4–Zr 2.261(4); P1–Pd–P2 99.7(1), O2–Pd–O4 75.1(1), O1A–Zr–O2 71.2(1), O3–Zr–O4 70.9(1), O2–Zr–O4 66.8(1).

atoms O2 and O4 is less pronounced than in the other complexes (sum of bond angles 346–351°) and induces in this case a folding of the ZrO₂Pd ring by 30° along the O2–O4 vector, whereas the zirconium biscatecholate moiety remains almost planar. The alignment of the two four-membered ZrO₂Pd rings (as defined by the interplanar angle between the O2–Zr–O4 and O2A–Zr–O4A planes) and the coordination planes of the two palladium atoms is close to orthogonal (interplanar angles 86°).

In addition to qualitative comparisons of the local environments of the individual templates, structure correlation between complexes **6–9** allows the specific influence of the template on the palladium coordination geometry to be analyzed further in a more quantitative fashion. The data shown in Table 1 and Figure 5 demonstrate that in the complexes **6–8**, each containing a single bisphosphine-palladium moiety, the observed lengthening of E–O distances to both terminal and bridging oxygen atoms closely mirrors the increase in the covalent radii of the template elements. Increasing the size (and the coordination number) of the template in turn induces an eventual widening of the O–Pd–O angle and simultaneous contraction of the P–Pd–P angle (with the sum of both angles remaining nearly constant in the range from 174.8° (**9**) to 176.8° (**8**)). The resulting structural changes may, in a simple picture, be described in terms of moving two rigid O,P-chelating functional phosphine ligands around an axis aligned perpendicular to the palladium coordination plane. The template thus acts as a lever that allows the P–Pd–P bond angle and the P···P distance to be tuned by adjustment of the arrangement of the μ₂-O donor atoms. The total magnitude of the actually observed structural changes in **6–8** amounts to a variation of 5° in P–Pd–P angles and 0.1 Å in P···P distances and so is similar to the variation ranges of some 4° in natural bite angles in a family of molecular bisphospholane ligands in which the geometric disposition of the P–C–C–P backbone was controlled through the incorporation of different rigid carbo- or heterocyclic rings,^[28] or in a series of Xantphos derivatives.^[29] In comparing these variations, however, it must be considered that the distinct preference of Pd^{II} for a square-planar coordination geometry imposes a strong restraint on the structural changes in **6–8**, thus implying that the potential variability in the supramolecular frameworks studied may be still larger.

The zirconium complex **9** supports a slightly larger P–Pd–P angle, as would be expected from correlation with the other complexes. This deviation is obviously related to the observed nonplanarity of the central ZrO₂Pd ring and is tentatively explained by the assumption that the interlocking of two different bisphosphine-palladium fragments on the same template enforces nearly parallel alignment of the two catecholate anchors of each binding pocket for steric reasons, and that the geometric constraints of the ligand backbone then force the palladium atom out of this plane. In contrast, the lower degrees of crowding around the template centers in **6–8** permit marked torsion of the catecholates, thus allowing the four-membered EO₂P chelate rings to remain planar and to act as structural directors.

Table 1. Comparison of covalent radii and coordination numbers of the template atom with observed average interatomic distances [Å] and angles [°] for **6–9**.

E	$r_{\text{cov}}^{[a]}$	C.N. ^[b]	E–O ^[c]	E–(μ_2 -O) ^[c]	P...P	P–Pd–P	O–Pd–O
7	Ga	1.25	5	1.898	2.027	3.489	101.8(1)
6	Sn	1.40	6	2.033	2.171	3.419	98.8(1)
9	Zr	1.45	8	2.145	2.276	3.404	99.7(1)
8	Bi	1.52	7	2.173	2.448	3.380	97.1(1)

[a] Data from ref. [30]. [b] C.N.=effective coordination number, including a lone pair for Bi^{III}. [c] Average over all crystallographically inequivalent bonds.

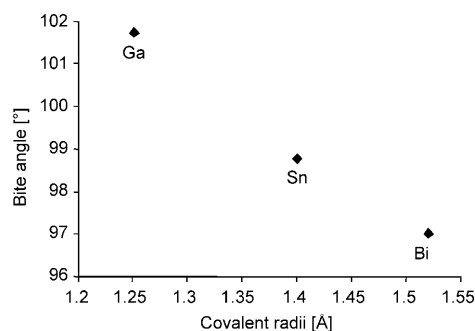


Figure 5. Correlation between covalent radius of the main group element template and P–Pd–P bite angle in **6–8**.

Although the reason for the formation of a trinuclear complex with two bisphosphine palladium units on a central zirconium template rather than a binuclear species of composition $[\text{Cl}_2\text{Zr}(\text{L})_2\text{Pd}]$ cannot be given with absolute confidence, we suggest that it lies in a combination of the high charge and large radius of the zirconium template. The space around the smaller tin atom is thus apparently insufficient to allow replacement of two chlorides by a second L_2Pd unit, which would boost the coordination number to eight. Bismuth(III) is larger but may still avoid a formal coordination number of nine (including the lone pair) because of space restrictions; furthermore, formation of a trinuclear BiPd_2 complex would result in the formation of an anionic species and thus violate the obviously preferred formation of neutral assemblies.

NMR studies: In addition to serving for the characterization of the complexes **6–9**, solution NMR data give insight into their dynamic behavior and solvation and thus complement information derived from the ESI-MS studies. The ^{31}P NMR signals of all complexes are in general characterized by substantial deshieldings, which have also been observed for other palladium complexes of phosphinoalcohols with five-membered chelate rings.^[22,31] The spectra of DMF solutions of **7** and **9** display sharp lines at chemical shifts of δ 65.0 and 52.4 ppm, respectively. The spectrum of **8** contains two broad signals at 70.8 ppm and 52.1 ppm, whereas **6** displays a single broad line at ambient temperature, which splits at lower temperature to give two signals of unequal intensity with chemical shifts of 77 ppm and 53 ppm (Figure 6). The temperature-dependent changes in relative signal intensities and the observed coalescence at high temperatures confirm

the assignment of the signals to two different species that undergo mutual chemical exchange. The same interpretation also holds for **8**, in which the presence of an exchange equilibrium follows from the observation that the single set

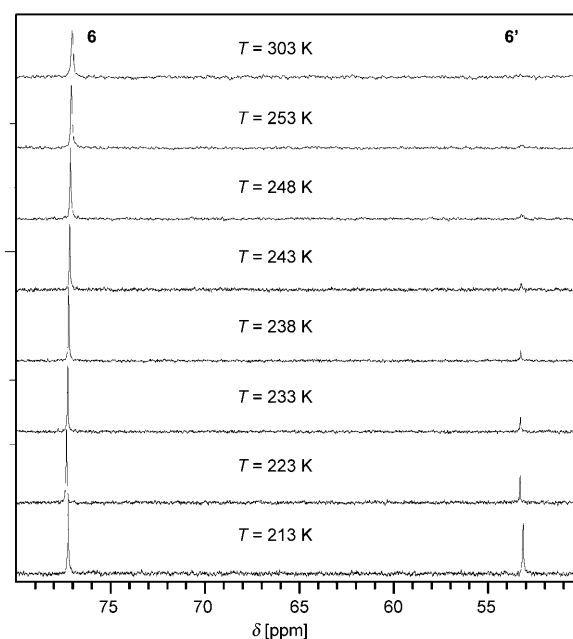
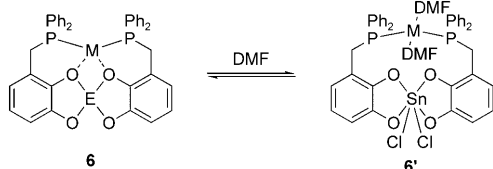


Figure 6. $^{31}\text{P}\{^1\text{H}\}$ NMR spectra of **6/6'** recorded between +30 and -60°C .

of (average) signals visible in the room-temperature ^1H NMR spectrum decoalesces into two signal sets at lower temperatures.

A detailed investigation of the dynamic process was carried out for **6** (a similar evaluation of the spectra of **8** was prevented by the fact that the large linewidth of the minor signal over the whole available temperature range prevented reliable quantification of relative signal intensities). Measurement of 2D ^{31}P EXSY spectra revealed that the dynamic exchange between the two observable species **6** and **6'** in DMF persists even at -55°C .^[32] Evaluation of the temperature dependence of the signal intensities was performed under the assumption that the exchange represents a pseudo-unimolecular reaction between two species determined by an equilibrium constant $K = [\mathbf{6}']/[\mathbf{6}]$, which allowed values of $\Delta H = -5.4 \text{ kcal mol}^{-1}$ and $\Delta S = -26 \text{ cal mol}^{-1} \text{ K}^{-1}$ to be extracted for the exchange process. The observation of two signals with chemical shifts similar to those seen in DMF was also observed in DMSO at ambient temperature, but not for solutions of **6** in noncoordinating solvents. Altogether, the observed phenomena can be interpreted by assuming that the second species **6'** is formed by coordination of extra solvent molecules, and it had been suggested from

the results of DFT calculations^[12] that the molecular structure of this species is most likely represented by a macrocyclic complex as shown in Scheme 3, in which the μ_2 -bridging oxygen atoms at palladium have been displaced by two newly incorporated solvent molecules. The observed temperature dependence of the equilibrium $[6']/[6]$ indicates that the solvent adduct is energetically more favorable than the solvent-free complex but that its formation is disfavored by entropy. In view of the easy displacement of the catechol oxygens from palladium, **6** can be seen as containing a hemi-



Scheme 3. Equilibrium between solvent-containing and solvent-free complexes **6** and **6'**.

labile ligand that can switch between tetradentate O_2P_2 - and bidentate P_2 -coordination. The catalytic potential of this complex in a C–C coupling reaction was demonstrated in a preliminary communication of this work.^[12] In regard of the facts that i) the observed ^{31}P NMR chemical shift of **9** in DMF or DMSO is similar to that of **6'** (and **8'**), and ii) the ESI-MS gives evidence for solvent coordination, it can be speculated that a solvent complex formed by cleavage of $(\mu_2-O)-Pd$ interaction is in this case the dominant species present in the solution.

At ambient temperature the 1H NMR spectra of **6–9** each display a single set of signals that exhibit chemical shifts similar to those seen in free **1**. The signals of **6–8** exhibit substantial line broadening, which arises from dynamic processes that lead at low temperatures to the occurrence of more complicated signal splittings. All compounds show eventual decoalescence of the signals of the phenyl protons into two sets of equally intense multiplets, and also of the doublet of the benzylic protons into a characteristic pattern of an ABX ($X = ^{31}P$) spin system; furthermore, in the case of **6**, additional signals attributable to **6'** (vide supra) become visible. Such a phenomenon is also noted for the bismuth complex **8**, although the presence of a second species **8'** is here only manifested in the appearance of an additional benzylic resonance; the remaining signals are presumably obscured by superposition with the much more intense ones of **8**.

The observation of two distinguishable phenyl moieties and an ABX pattern for the benzylic protons of **6–8** at low temperature reflect the anisochronicity of the nuclei in the μ -bridging CH_2PPh_2 moieties, which arises from the fact that in these molecules the chelating coordination by two catecholate ligands renders the coordination sphere of the template E chiral. The coalescence of these signals with increasing temperature is then due to racemization of this chiral coordination sphere. Since the persistence of the $J_{P,Sn}$ coupling in a similar template complex $[Pd(L)_2SnMe_2]$ indicates that

the binuclear framework remains kinetically stable,^[12] the racemization must be considered an intramolecular process. Possible mechanisms involve inversion of the chiral octahedron analogously with the Bailar-twist mechanism,^[33] but a more complicated, solvent-assisted mechanism involving intermediate opening of a catechol-chelate ring (e.g., induced by protonation through traces of H_2O present in the solutions) cannot be ruled out. Although the dynamic stereochemistry of Sn-catecholates has not been studied in detail, it is known that catechol phosphates may racemize very easily,^[34] and the observed behavior of **6** adheres to this pattern.

The 1H NMR signals of the benzylic protons of the solvent adduct **6'** (and **8'**) identified at low temperature give no evidence of splitting, indicating the chemical inequivalence of the two protons. If one considers, however, that these signals remain broad even at the lowest accessible temperature, it is currently unclear whether this is due to failure to reach the slow-exchange regime (either because of accidental near-degeneracy of the chemical shifts at the exchanging sites, or because of a still lower energetic barrier for the racemization process), or whether the molecular structure of this species is achiral, thus leaving the geminal protons chemically equivalent.

Some further interesting information was obtained from solid-state NMR spectra of a DMF solvate of **6** obtained by precipitation of the complex from DMF. The $^{31}P\{^1H\}$ CP-MAS spectrum shows two signals at $\delta_{iso} = 79.5$ and 74.1 ppm, which in a J -resolved 2D spectrum display a coupling of $^2J_{P,P} = 41$ Hz and clearly indicate the presence of an AB spin system with two inequivalent phosphorus atoms. A likely explanation for this observation is that **6**-DMF forms a pseudo-polymorph of the dichloromethane solvate that was characterized by X-ray diffraction, and that the crystallographic equivalence of the phosphorus atoms in the former is lost. The ^{119}Sn CP-MAS NMR spectrum of the solid sample shows an isotropic line at $\delta_{iso} = -455$ ppm, indicating the presence of only one ^{119}Sn site. The observed isotropic ^{31}P chemical shifts match the solution value of $\delta(^{31}P)$ assigned to **6**, but differ from that of **6'**, thus suggesting that the μ -bridging coordination of the oxygen atoms is maintained. The CP-MAS spectra, like the X-ray diffraction study, give no evidence of the presence of a species such as **6'** in the solid state.

Conclusion

Application of the concept of preparing metal complexes with chelating, template-centered bisphosphine ligands by self-assembly of simple hard and soft metal complex precursors with bifunctional phosphine-catecholate ligands in a single synthetic step has served for the successful assembly of a series of palladium complexes on different triply or quadruply charged main group metal ions as template. In addition, a trinuclear complex featuring two palladium bisphosphine moieties on a central transition metal (Zr) tem-

plate was obtained by the same approach. The reported reactions differ from known synthetic strategies in requiring neither the dedicated synthesis of a polydentate chelate ligand,^[35] nor the need for introducing the metal atoms in separate reaction steps,^[36] but may be considered the first examples of a family of complexes with supramolecular ligands assembled on main group element templates. Correlation of the structural features of these complexes demonstrates that the choice of templates of different size and coordination number permits the steric bulk and the P-Pd-P bite angle of the chelating bisphosphine unit to be adjusted in a predictable manner and through a tuning range similar to those available by structural variation of the backbones in molecular bisphosphine complexes. Furthermore, the template-centered assembly is robust enough to endure the displacement of the μ_2 -bridging oxygen donor atoms by suitable solvent molecules, thus mimicking the behavior of a hemilabile ligand. In view of the fact that the catalytic activity of **6** has already been demonstrated,^[12] the special combination of tunable steric requirements and hemilabile behavior offer promising prospects for the application of the reported complexes and of similar derivatives assembled on other main group or transition metal elements in catalysis.

Experimental Section

General remarks: All manipulations were carried out under dry argon with use of standard Schlenk techniques. Solvents were dried by standard procedures^[37] unless otherwise mentioned. The catechol phosphine **1** was prepared as reported earlier.^[10] [(cod)PdCl₂] was prepared as described in the literature;^[38] GaCl₃, SnCl₄, ZrCl₄, Cs₂CO₃, and triethylamine were commercially available and were used without further purification. NMR spectra were recorded on a Bruker Avance 400 spectrometer (¹H: 400.1 MHz, ¹³C: 100.5 MHz, ³¹P: 161.9 MHz) at 303 K unless mentioned otherwise; chemical shifts are referenced to external TMS (¹H, ¹³C) or 85% H₃PO₄ (Ξ = 40.480747 MHz, ³¹P). Solid-state MAS-NMR spectra were recorded with spinning speeds between 3 to 14 kHz. Cross polarization with a ramp-shaped contact pulse and mixing times of between 3 and 5 ms were used for signal enhancement in CP/MAS experiments. Coupling constants are given as absolute values; prefixes *i*, *o*, *m*, and *p* denote phenyl ring positions of P-C₆H₅ substituents, C₆H₅ represents the catechol ring protons. The ¹H NMR assignments in the cases of **6/6'** and **8/8'** were derived from ¹H-COSY, ¹H-NOESY, and ³¹P-HMQC NMR spectra. EI-MS: Varian MAT 711, 70 eV. ESI-MS: Bruker Daltonics microTOF-Q. Elemental analysis: Perkin-Elmer 24000CHN/O Analyzer; large deviations from calculated values in the case of solvates are attributable to the presence of nonstoichiometric amounts of solvent. Melting points were determined in sealed capillaries.

Complex 6: A mixture of **1** (600 mg, 1.95 mmol), SnCl₄ (1.1 mL, 0.97 mmol), [(cod)PdCl₂] (280 mg, 0.97 mmol), and NEt₃ (0.8 mL, 5.7 mmol) in dry DMF (20 mL) was stirred for 24 h at 60 °C. The red suspension was filtered through a bed of celite. The filtrate was evaporated in vacuum, and the residue was washed with CH₂Cl₂ (10 mL) and dissolved in little DMF. The same volume of CH₂Cl₂ and, finally, small portions of Et₂O were added until a precipitate began to form. The mixture was stored overnight at +4 °C to yield a microcrystalline solid, which was collected by filtration and dried in vacuum for 4 h at 70 °C to yield **6** (60%) of m.p. 214 °C (decomp). ¹H NMR ([D₇]DMF): δ = 7.70 to 7.25 (brm, 20H; P-C₆H₅), 6.90 (d, ³J_{HH} = 8.0 Hz, 2H; C₆H₅), 6.58 (brs, 2H; C₆H₅), 6.10–6.03 (brs, 2H; C₆H₅), 4.0 to 3.7 ppm (br, 4H; CH₂); ³¹P{¹H} NMR ([D₇]DMF): δ = 77.0 ppm (brs); ³¹P{¹H} CP-MAS NMR: δ_{iso} = 79.5, 74.1 ppm; J_{PP} = 41 Hz (2D *J*-resolved); ¹¹⁹Sn{¹H} CP-MAS

NMR: δ_{iso} = -455; elemental analysis (%) calcd for C₃₈H₃₀Cl₂O₄P₂PdSn (908.64): DMF: C 50.16, H 3.80, N 1.43; found: C 49.92, H 3.77, N 1.58.

Low-temperature NMR study of compound 6/6': ¹H NMR ([D₇]DMF, 223 K): δ = 7.87, 7.73, 7.62 (all br, 10H; P-C₆H₅), 7.57, 7.43, 7.28 (all br, 10H; P-C₆H₅), 6.93 (d, 2H; C₆H₅), 6.55 (t, 2H; C₆H₅), 5.98 (d, 2H; C₆H₅), 4.64 (m, 2H; PCH₂), 3.86 ppm (m, 2H; PCH₂); ³¹P{¹H} NMR ([D₇]DMF, 223 K): δ = 77.0 ppm (brs). **Compound 6':** ¹H NMR ([D₇]DMF, 223 K): δ = 7.74, 7.68, 7.43 (all br, 20H; C₆H₅), 7.6–6.5 (br, 6H; C₆H₅), 4.16 ppm (br, 4H; PCH₂); ³¹P{¹H} NMR ([D₇]DMF, 223 K): δ = 55.5 ppm (brs).

Complex 7: Phosphine **1** (400 mg, 1.29 mmol), GaCl₃ (114 mg, 0.64 mmol), [(cod)PdCl₂] (185 mg, 0.64 mmol), and triethylamine (0.5 mL, 3.2 mmol) were placed in a dried 100 mL Schlenk tube, dry DMF (10 mL) was added, and the reaction mixture was stirred at room temperature for 3 h. The formed mixture was filtered through a glass frit, and the filtrate was evaporated to dryness in vacuum. The red powder was again dissolved in DMF (10 mL), the solution was diluted with Et₂O (80 mL), and the formed precipitate was collected by filtration. This procedure was repeated one more time, and the remaining residue was then dried in vacuum at 70 °C to give **7** (369 mg, 70%) with m.p. 358 °C. Single crystals were obtained by recrystallization of a sample from CHCl₃. ¹H NMR (CDCl₃): δ = 7.75–6.95 (m, 20H; Ph), 6.60 (d, ³J_{HH} = 6.8 Hz; C₆H₅), 6.47 (t, ³J_{HH} = 7.8 Hz; C₆H₅), 6.24 (d, ³J_{HH} = 7.5 Hz; C₆H₅), 3.78–3.66 ppm (brs; CH₂); ¹³C{¹H} NMR (CDCl₃): δ = 153.2 (m; C₆H₅), 146.6 (m; C₆H₅), 133.0 (m, ΣJ_{FC} = 8.9 Hz, *m*-C, P-C₆H₅), 132.3 (m; P-C₆H₅), 129.4–128.6 (m; P-C₆H₅), 119.9 (m; C₆H₅), 118.3 (t, J_{PC} = 1.3 Hz), 116.4 (ddd, ΣJ_{PC} = 3.4 Hz; C₆H₅), 113.3 (m; C₆H₅), 31.9 ppm (m, CH₂); ³¹P{¹H} NMR (CDCl₃): δ = 65.3 ppm (s); ESI-MS (positive mode): *m/z*: 825.0 [M+H]⁺, 847.0 [M+Na]⁺, 857.0 [M+CH₃OH+H]⁺; ESI-MS (negative mode): *m/z*: 823.0 [M-H]⁻, 856.9 [M+Cl]⁻; elemental analysis (%) calcd for C₃₈H₃₀ClGaO₄P₂Pd (824.17): C 55.38, H 3.67; found: C 53.02, H 3.50

Complex 8: Dry DMF (8 mL) was added to a mixture of **1** (280 mg, 0.90 mmol), BiCl₃ (143 mg, 0.45 mmol), [(cod)PdCl₂] (130 mg, 0.45 mmol), and triethylamine (0.32 mL, 2.3 mmol), and the resulting mixture was stirred at room temperature for 3 h. The dark-red suspension was filtered through a glass frit, and the filtrate was kept at -28 °C overnight. White, needle-like crystals of triethylammonium chloride formed and were decanted off. Dilution of the filtrate with excess Et₂O produced a precipitate, which was dried in vacuum and recrystallized from CH₂Cl₂ to produce **8** (303 mg, 70%) with m.p. 273 °C. Single crystals were grown from a concentrated CH₂Cl₂ solution at room temperature. ¹H NMR ([D₇]DMF): δ = 7.9–7.2 (m, 20H; P-C₆H₅), 6.8–6.1 (brs, 6H; C₆H₅), 6.0 (s, 2H; CH₂Cl₂), 3.9–3.70 ppm (brd, 4H; CH₂); ³¹P{¹H} NMR ([D₇]DMF): δ = 70.8 (brs), 52.1 ppm (brs); ESI-MS (positive mode): *m/z*: 927.0 [M-Cl]⁺, 969.0 [M+L]⁺; elemental analysis (%) calcd for C₃₈H₃₀BiClO₄P₂Pd (963.45)-CH₂Cl₂: C 44.68, H 3.08; found: C 44.51, H 3.03.

Low-temperature study of complex 8: ¹H NMR ([D₇]DMF, 223 K): δ = 8.03–7.90 (br; *o*-C₆H₅), 7.74 (t, ³J_{HH} = 7.0 Hz; P-C₆H₅), 7.64 (t, ³J_{HH} = 6.6 Hz; P-C₆H₅), 7.54 (t, ³J_{HH} = 7.1 Hz; P-C₆H₅), 7.31 (t, ³J_{HH} = 7.2 Hz; P-C₆H₅), 7.22–7.12 (brm, P-C₆H₅), 6.64 (t, ³J_{HH} = 7.4 Hz; C₆H₅), 6.49 (d, ³J_{HH} = 7.2 Hz; C₆H₅), 6.28 (d, ³J_{HH} = 7.0 Hz; C₆H₅), 6.22 (s; CH₂Cl₂), 3.91 (brm; CH₂), 3.76 ppm (d, ²J_{PH} = 11.2 Hz; CH₂); ³¹P{¹H} NMR ([D₇]DMF, 223 K): δ = 69.8 (s), 50.4 ppm (s).

Complex 9: A mixture of **1** (200 mg, 0.64 mmol), ZrCl₄ (76 mg, 0.32 mmol), [(PhCN)₂PdCl₂] (124 mg, 0.32 mmol), and Cs₂CO₃ (423 mg, 1.3 mmol) was placed in a Schlenk tube. The solid mixture was dissolved in DMF (15 mL) and stirred for 6 d at room temperature. The red suspension was filtered, and the filtrate was evaporated to dryness. The red residue was dissolved in DMF/CH₂Cl₂ (1:1) and diluted with Et₂O (50 mL). The formed precipitate was filtered off and dried in vacuum to produce **9** (293 mg, 60%) with m.p. 390 °C (decomp). An analytically pure sample was prepared by slow diffusion of Et₂O into a concentrated DMSO solution, and single crystals suitable for X-ray diffraction were prepared in the same manner starting from a solution in DMF. ¹H NMR ([D₆]DMSO): δ = 7.53 (t, ³J_{PH} = 8.72 Hz, 16H; P-C₆H₅), 7.36 (t, ³J_{HH} = 7.3 Hz, 8H; P-C₆H₅), 7.15 (t, ³J_{HH} = 6.8 Hz, 16H; P-C₆H₅), 6.0–6.2 (m,

8H; C₆H₃), 5.97 (d, ³J_{H,H} = 7.1 Hz, 4H; C₆H₃), 3.64 ppm (br, 8H; CH₂); ³¹P{¹H} NMR ([D₆]DMSO): δ = 52.4 ppm (s); ESI-MS (positive mode): m/z: 1713.0 [M+2DMF+K]⁺; elemental analysis (%) calcd for C₇₆H₆₀O₈P₄Pd₂Zr·3DMSO: C 55.85, H 4.46; found: C 55.38, H 4.40.

Crystal structure determinations of 6–9: Crystallographic data were collected on Bruker–Nonius Kappa CCD (8), Nonius Kappa CCD (9), or Siemens P3 (7) or P4 (6) diffractometers at 100(2) K (9), 123(2) K (8), or 173(2) K (6, 7) with use of Mo–K_α radiation (λ = 0.71073 Å). Direct Methods (SHELXS-97^[39]) were used for structure solution and refinement (SHELXL-97^[40] full-matrix, least-squares on F²). Hydrogen atoms were refined with a riding model. The contributions of two severely disordered dichloromethane or DMF molecules in solvent-accessible cavities of 6 and 9, respectively, were eliminated from the reflection data by use of the BYPASS^[41] method as implemented in the SQUEEZE routine of the PLATON98 package.

Complex 6: Red crystals, C₃₈H₃₀Cl₂O₄P₂PdSn·3CH₂Cl₂, M = 908.56, crystal size 0.40 × 0.15 × 0.08 mm, monoclinic, space group P₂/c (No. 13): a = 12.227(2), b = 11.707(2), c = 16.475(3) Å, β = 102.516(12)°, V = 2302.2(7) Å³, Z = 2, ρ_{calcd} = 1.311 Mg m⁻³, F(000) = 900, μ = 1.149 mm⁻¹, semiempirical absorption correction by use of Ψ scans, min/max. abs. 0.600/0.793, 6056 reflexes (2θ_{max} = 56.0°), 5523 unique [R_{int} = 0.024], 220 parameters, R1 (I > 2σ(I)) = 0.0445, wR2 (all data) = 0.1248, largest diff. peak and hole 1.94 and -1.08 e Å⁻³.

Complex 7: Dark red crystals, C₃₈H₃₀ClGaO₄P₂Pd·3CHCl₃, M = 1182.23, crystal size 0.35 × 0.30 × 0.15 mm, monoclinic, space group P₂/n (No. 14): a = 16.125(4), b = 14.211(4), c = 21.533(5) Å, β = 106.642(19)°, V = 4728(2) Å³, Z = 4, ρ_{calcd} = 1.661 Mg m⁻³, F(000) = 2352, μ = 1.623 mm⁻¹, semiempirical absorption correction by use of Ψ-scans, min/max. abs. 0.589/0.923, 10672 reflexes (2θ_{max} = 54.0°), 10308 unique [R_{int} = 0.0497], 535 parameters, 0 restraints, R1 (I > 2σ(I)) = 0.0514, wR2 (all data) = 0.1148, largest diff. peak and hole 0.79 and -0.89 e Å⁻³.

Complex 8: Dark red crystals, C₃₈H₃₀BiClO₄P₂Pd·CH₂Cl₂, M = 1048.32, crystal size 0.15 × 0.06 × 0.04 mm, monoclinic, space group P₂/c (No. 14): a = 12.264(1) Å, b = 17.247(1) Å, c = 19.346(1) Å, β = 98.52(1)°, V = 3716.9(4) Å³, Z = 4, ρ_{calcd} = 1.873 Mg m⁻³, F(000) = 2032, μ = 5.554 mm⁻¹, semiempirical absorption correction from multiple reflections, min/max. abs. 0.458/0.808, 21315 reflexes (2θ_{max} = 50°), 6485 unique [R_{int} = 0.0695], 451 parameters, R1 (I > 2σ(I)) = 0.0472, wR2 (all data) = 0.0978, S = 1.033, largest diff. peak and hole 2.226 and -0.989 e Å⁻³.

Complex 9: Red crystals, C₇₆H₆₀O₈P₄Pd₂Zr·4.5DMF, M = 1858.07, crystal size 0.35 × 0.20 × 0.20 mm, monoclinic, space group C₂/c (No. 15): a = 25.0208(7), b = 15.3922(5), c = 25.6866(5) Å, β = 107.045(2)°, V = 9458.0(4) Å³, Z = 4, ρ_{calcd} = 1.305 Mg m⁻³, F(000) = 3808, μ = 0.609 mm⁻¹, 38069 reflexes (2θ_{max} = 50°), 8189 unique [R_{int} = 0.095], 505 parameters, R1 (I > 2σ(I)) = 0.0629, wR2 (all data) = 0.1545, S = 1.038, largest diff. peak and hole 1.028 and -0.598 e Å⁻³.

Crystallographic data (excluding structure factors): CCDC 616084 (6), CCDC 695488 (7), CCDC 694126 (8), and CCDC 694127 (9) contain the supplementary crystallographic data for this paper. These data can be obtained free of charge from The Cambridge Crystallographic Data Centre via www.ccdc.cam.ac.uk/data_request/cif.

Acknowledgements

We thank Dr. J. Opitz, J. Trinkner, and K. Wohlbold (Institut für Organische Chemie, Universität Stuttgart) for recording the mass spectra. The Deutsche Forschungsgemeinschaft is acknowledged for financial support.

- [1] a) V. F. Slagt, P. W. N. M. van Leeuwen, J. N. H. Reek, *Chem. Commun.* **2003**, 2474–2475; b) P. Braunstein, G. Clerc, X. Morise, R. Welter, G. Mantovani, *Dalton Trans.* **2003**, 1601–1605; c) J. M. Takacs, D. S. Reddy, S. A. Moteki, D. Wu, H. Palencia, *J. Am. Chem. Soc.* **2004**, *126*, 4494–4495; d) B. Breit, *Angew. Chem.* **2005**, *117*, 6976–6986; *Angew. Chem. Int. Ed.* **2005**, *44*, 6816–6825; e) A. J. Sandee, J. N. H. Reek, *Dalton Trans.* **2006**, 3385–3391.

- [2] C. A. Tolman, *Chem. Rev.* **1977**, *77*, 313–348; P. W. N. M. van Leeuwen, P. C. J. Kamer, J. N. H. Reek, P. Dierkes, *Chem. Rev.* **2000**, *100*, 2741–2769; P. W. N. M. van Leeuwen, P. C. J. Kamer, J. N. H. Reek, *Pure Appl. Chem.* **1999**, *71*, 1433–1452.
- [3] See for examples: P. J. Pye, K. Rossen, R. A. Reamer, N. N. Tsou, R. P. Volante, P. J. Reider, *J. Am. Chem. Soc.* **1997**, *119*, 6207–6208; P. J. Pye, K. Rossen, R. A. Reamer, N. N. Tsou, R. P. Volante, P. J. Reider, *Tetrahedron Lett.* **1998**, *39*, 4441–4444; M. van den Berg, A. J. Minnaard, E. P. Schudde, J. van Esch, A. H. M. de Vries, J. G. de Vries, B. L. Feringa, *J. Am. Chem. Soc.* **2000**, *122*, 11539–11540; M. T. Reetz, G. Mehler, *Angew. Chem.* **2000**, *112*, 4047–4049; *Angew. Chem. Int. Ed.* **2000**, *39*, 3889–3890.
- [4] R. Kranich, K. Eis, O. Geis, S. Muhle, J. W. Bats, H.-G. Schmalz, *Chem. Eur. J.* **2000**, *6*, 2874; F. Blume, S. Zemolka, T. Fey, R. Kranich, H.-G. Schmalz, *Adv. Synth. Catal.* **2002**, *344*, 868; J. Holz, O. Zayas, H. Jiao, W. Baumann, A. Spannenberg, A. Monsees, T. H. Riermeier, J. Almena, R. Kadyrov, A. Börner, *Chem. Eur. J.* **2006**, *12*, 5001.
- [5] Reviews: ref. [1d]; A. J. Sandee, J. N. H. Reek, *Dalton Trans.* **2006**, 3385–3391.
- [6] B. Breit, W. Seiche, *Angew. Chem.* **2005**, *117*, 1666–1669; *Angew. Chem. Int. Ed.* **2005**, *44*, 1640–1643; C. Waloch, J. Wieland, M. Keller, B. Breit, *Angew. Chem.* **2007**, *119*, 3097–3099; *Angew. Chem. Int. Ed.* **2007**, *46*, 3037–3039.
- [7] V. F. Slagt, P. C. J. Kamer, P. W. N. M. van Leeuwen, J. N. H. Reek, *Angew. Chem.* **2001**, *113*, 4401–4404; *Angew. Chem. Int. Ed.* **2001**, *40*, 4271–4274; V. F. Slagt, P. C. J. Kamer, P. W. N. M. van Leeuwen, J. N. H. Reek, *J. Am. Chem. Soc.* **2004**, *126*, 1526–1536.
- [8] J. M. Takacs, K. Chaiseeda, S. A. Moteki, D. S. Reddy, D. Wu, K. Chandra, *Pure Appl. Chem.* **2006**, *78*, 501–509; S. A. Moteki, J. M. Takacs, *Angew. Chem.* **2008**, *120*, 908–911; *Angew. Chem. Int. Ed.* **2008**, *47*, 894–897.
- [9] P. A. Duckmanton, A. J. Blake, J. B. Love, *Inorg. Chem.* **2005**, *44*, 7708–7710; L. K. Knight, Z. Freixa, P. W. N. M. van Leeuwen, J. N. H. Reek, *Organometallics* **2006**, *25*, 954–960.
- [10] S. Chikkali, D. Gudat, *Eur. J. Inorg. Chem.* **2006**, 3005–3009.
- [11] S. H. Chikkali, D. Gudat, F. Lissner, M. Nieger, T. Schleid, *Dalton Trans.* **2007**, 3906–3913.
- [12] S. Chikkali, D. Gudat, M. Niemeyer, *Chem. Commun.* **2007**, 981–983.
- [13] C. Lamberth, J. C. Machell, D. M. P. Mingos, T. L. Stolberg, *J. Mater. Chem.* **1991**, *1*, 775, and cited refs.
- [14] G. Smith, A. N. Reddy, K. A. Byriell, C. H. L. Kennard, *Aust. J. Chem.* **1994**, *47*, 1413–1418.
- [15] T. J. Boyle, L. J. Tribby, T. M. Alam, S. D. Bunge, G. P. Holland, *Polyhedron* **2005**, *24*, 1143–1152.
- [16] B. Kersting, J. R. Relford, M. Meyer, K. N. Raymond, *J. Am. Chem. Soc.* **1996**, *118*, 5712–5721; M. Meyer, B. Kersting, R. E. Powers, K. N. Raymond, *Inorg. Chem.* **1997**, *36*, 5179–5191.
- [17] T. B. Karpishin, T. M. Dewey, K. N. Raymond, *J. Am. Chem. Soc.* **1993**, *115*, 1842–1851.
- [18] C. N. R. Rao, B. Raveau, *Transition Metal Oxides*, VCH, New York, **1995**; K. G. Caulton, L. G. Hubert-Pfalzgraf, *Chem. Rev.* **1990**, *90*, 969–995; D. Villemin, P. A. Jaffres, B. Nechab, F. Courivaud, *Tetrahedron Lett.* **1997**, *38*, 6581–6584; M. Xuebing, F. Xiangkai, *J. Mol. Catal. A* **2004**, *208*, 129–133.
- [19] H. Ishii, M. Ueda, K. Takuechi, M. Asai, *J. Mol. Catal. A* **1999**, *138*, 311.
- [20] Given numbers refer to the mass of the most abundant isotopomer. The suggested elemental composition was in all cases confirmed by comparison of observed and simulated isotope patterns.
- [21] Mean Pd–P distance and standard deviation as found in a query in the CSD data base for complexes of the type *cis*-[Cl₂Pd(PR₃)₂].
- [22] J. S. Kim, A. Sen, I. A. Guzei, L. M. Liable-Sands, A. L. Rheingold, *J. Chem. Soc. Dalton Trans.* **2002**, 4726–4732.
- [23] A CSD query for the sums of bond angles in complexes containing μ₂-bridging phenolate ligands returned a mean value and standard deviation of 354 ± 9°, with a maximum of the distribution at 360°.

- [24] See for example: B. A. Borgias, S. J. Barclay, K. N. Raymond, *J. Coord. Chem.* **1986**, *15*, 109–123; M. A. Brown, A. A. El-Hadad, B. R. McGarvey, R. C. W. Sung, A. K. Trikha, D. G. Tuck, *Inorg. Chim. Acta* **2000**, *300*, 613–621.
- [25] C. N. McMahon, S. J. Obrey, A. Keys, S. G. Bott, A. R. Barron, *J. Chem. Soc. Dalton Trans.* **2000**, 2151–2161; N. R. Bunn, S. Aldridge, C. Jones, *Appl. Organomet. Chem.* **2004**, *18*, 425–426.
- [26] A. Kempter, C. Gemel, R. A. Fischer, *Chem. Commun.* **2006**, 1551–1553; B. Buchin, C. Gemel, T. Cadenbach, R. A. Fischer, *Inorg. Chem.* **2006**, *45*, 1789–1794.
- [27] C. J. Gramer, K. N. Raymond, *Inorg. Chem.* **2004**, *43*, 6397–6402.
- [28] J. Holz, O. Zayas, H. Jiao, W. Baumann, A. Spannenberg, A. Monsees, T. H. Riermeier, J. Almena, R. Kadyrov, A. Börner, *Chem. Eur. J.* **2006**, *12*, 5001–5013.
- [29] M. Kranenburg, Y. E. M. van der Burgt, P. C. J. Kamer, P. W. N. M. van Leeuwen, K. Goubitz, J. Fraanje, *Organometallics* **1995**, *14*, 3081–3089.
- [30] J. D. Lee, *Concise Inorganic Chemistry V*, Blackwell, **1996**, p. 147.
- [31] D. J. Brauer, P. M. Machnitzki, T. Nickel, O. Stelzer, *Eur. J. Inorg. Chem.* **2000**, 65–73.
- [32] Attempts to characterize the observable species through additional ^{119}Sn NMR data failed because no signals were observable, due to the unfavorable combination of low solubility and dynamic line broadening.
- [33] D. Casanova, J. Cirera, M. Llunell, P. Alemany, D. Avnir, S. Alvarez, *J. Am. Chem. Soc.* **2004**, *126*, 1755–1763.
- [34] J. Lacour, C. Ginglinger, C. Grivet, G. Bernardinelli, *Angew. Chem.* **1997**, *109*, 660–662; *Angew. Chem. Int. Ed. Engl.* **1997**, *36*, 608–610, and references therein.
- [35] A. Kless, C. Lefeber, A. Spangenberg, R. Kempe, W. Baumann, J. Holz, A. Börner, *Tetrahedron* **1996**, *52*, 14599–14606.
- [36] G. S. Ferguson, P. T. Wolczanski, *J. Am. Chem. Soc.* **1986**, *108*, 8293–8295.
- [37] D. D. Perrin, W. L. Armarego, L. F. Willfred, *Purification of Laboratory Chemicals*, Pergamon, Oxford, **1988**.
- [38] P. M. Maitlis, *The Organic Chemistry of Palladium Metal Complexes, Vol. 1*, Academic Press, New York, **1971**, and references therein.
- [39] G. M. Sheldrick, *Acta Crystallogr. Sect. A* **2008**, *64*, 112–122.
- [40] G. M. Sheldrick, University Göttingen (Germany), **1997**.
- [41] P. van der Sluis, A. L. Spek, *Acta Crystallogr. Sect. A* **1990**, *46*, 194–201.

Received: July 25, 2008

Published online: November 26, 2008